JOURNAL OF APPLIED ELECTROCHEMISTRY 4 (1974) 7–16

Influence of cell geometry on the shape of polarization curves of porous Pt electrodes on a YSZ electrolyte

S. PIZZINI, M. BIANCHI, A. CORRADI AND C. MARI

Laboratory of Electrochemistry and Metallurgy, University of Milano, Via Venezian 21, Milan, Italy

Received 16 March 1973

The use of model electrochemical cells for the purpose of optimizing the design and performances of cells using a ceramic oxide electrolyte is considered. Measurements carried out on these cells are compared with results of polarization experiments with Pt electrodes on an yttria-stabilized zirconia electrolyte.

1. Introduction

In two previous papers [1, 2], which dealt with the general aspects of the kinetics of the oxygen reduction reaction at porous Pt electrodes, results of systematic polarization experiments carried out in our laboratory [3, 4] were discussed without direct reference to the experimental assembly. The present paper gives details of the experimental work for the different electrode/reference electrode/counter-electrode configurations used, in terms of model electrochemical cells [5].

The influence of the electrode/counter electrode configuration in electrochemical cells working at high temperatures has been often underestimated, despite much published evidence that it is of overwhelming importance, at least with conventional liquid electrolytes.

The details of recent experimental assemblies given in Table 1 show that different geometrical arrangements are often adopted only to accommodate the severe restrictions arising from the use of ceramic electrolytes of commercial sizes and shapes rather than for the optimization of experimental conditions. No one of these configurations is free from shortcomings, with the possible exception of those adopted by Kleitz [9], Guillou [10] Bauerle [11] and Schouler [12].

As an example, Kroger's configuration [6] does not permit the use of different gas atmospheres on the two sides of the electrolyte, and, like that used by Etsell and Flengas [7], does not give reliable results unless the counter/reference electrode is operated under conditions of zero overvoltage, i.e. at very low current levels.

The Karpachev cell [8] suffers from a different limitation, due to the fact that the current density is non-uniform as a consequence of the presence of the reference electrode (RE) on the opposite face of the pellet-type electrolyte, as shown in Fig. 1.

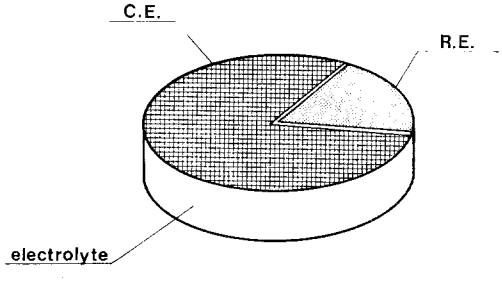

Fig. 1. Three-electrode polarization cell (*after* Karpachev *et al.* [8]).

Conversely, the point electrode type of electrode geometry originally used by Guillou *et al.* [10] and by Kleitz [9], provides a practically hemispherical distribution of the equipotential lines in the region of the electrolyte near to the

Table 1. Summary of cell configurations and electrode preparation procedures reported in the current literature

Authors	*Type of cell*	*Electrolyte*	*Electrodes*	*Electrode preparation*	*Type of polarization*
Kroger *et al.* [6]	1 compartment, 2 electrodes/cell	ZrO_2–CaO (85–15) tablet	One of *c.* 20 mm, one of *c.* 1 mm^2	From Pt paste fired at 800°C	Galvanostatic (with voltage divider)
Etsell and Flengas [7]	2 compartments, 2 electrodes/cell	Flat, closed end ZrO_2–CaO tube (90–10)	One of 1·15 cm^2, the counter one of 1·43 cm^2.	From chlor-platinic acid, fired at 1100°C	Galvanostatic (with voltage divider); the counter electrode also acts as reference
Karpachev *et al.* [8]	1 compartment, 3 electrodes cell	ZrO_2–Y_2O_3 (0·91–0·09) or ZrO_2–$ScO_{1.5}$ (88–12) tablets	The reference electrode is on the same side of the counter electrode	From chlor-platinic acid, fired at 600–700°C	Galvanostatic
Kleitz [9] Guillou *et al.* [10]	2 compartments, 2 electrodes cell tube	ZrO_2–CaO (85–15)	Working Pt wire, counter porous Pt	—	Galvanostatic
Bauerle [11]	1 compartment, 2 electrodes cell	ZrO_2–Y_2O_3 (90–10) tablets	Porous or sputtered Pt	From Pt paste or vacuum sputtered	Complex admittance method
Schouler [12]	1 compartment, 2 electrodes cell	Stabilized zirconia	Porous Pt electrodes	From Pt paste paste	Complex admittance method

electrode; a very convenient boundary condition for the solution of diffusion equations.

The determination of ohmic drop contributions to the overall overvoltage measured requires either the use of oscillographic, fast pulse methods or the complex admittance method first used by Bauerle and recently by Schouler [12].

To obtain the optimum cell configuration, the technique of model electrochemical cells has been used, which, with a simple experimental set-up, allows the location of the equipotential lines in the electrolyte and hence the mapping of the equipotential as well as the current flux lines. These maps make it possible either to adjust the electrode/counter-electrode configuration for better uniformity of the current lines at the electrode or to best locate the reference electrode, to minimize the contribution of ohmic drop to the overall overvoltage measured.

2. Model electrochemical cells: experimental layouts and results

These models, made of shaped conductive paper, are two-dimensional, enlarged (normally 20:1) sections of the three-dimensional systems shown in Figs. 2 and 3, which are examples of the cells most used in laboratory practice.

Copper plates, connected to a direct current source, were used to obtain the necessary good contact with the electrodes. Very small changes in the positions of the weights fixing the plates to the electrodes greatly affected the results. The equipotential lines could be drawn by reading the voltage drops between the electrode and a point on the surface via a probe, whilst a constant current (20 μA) was passing in the cell, as shown in Fig. 4.

In the case of parallel electrodes, the counter-electrode was maintained at the same diameter,

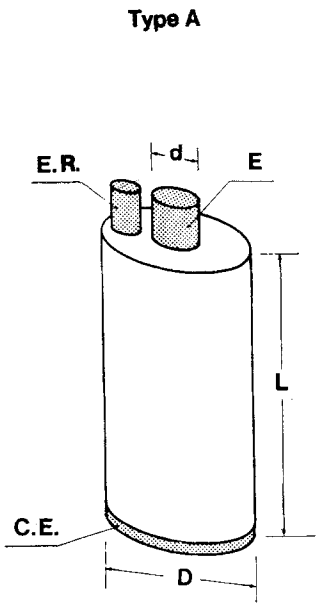

Fig. 2. Three-electrode polarization cell. E = electrode; ER = reference electrode; CE = counter electrode; D = electrolyte and counter electrode diameter; L = thickness of the electrolyte.

whilst the (upper) electrode was varied in size within fixed limits (see below). With more complicated cell geometries, as shown in Figs. 4b and 4c, the shape and the dimensions of the electrodes was varied within wide limits, which depend on the kind of electrodes to be used in real cells.

Figs. 5 and 6 give some results dealing with cells of the A-type. In Fig. 7 are results from cells of the B-type and in Figs. 8 and 9 data from cells of the C-type, with one- or two-ring electrodes on the lateral wall of a flat and closed end cylindrical tube are shown.

Analysis of the results shows the following:

1. Provided the diameter, d, of the electrode in type A cells is less than 1/6 of the diameter, D, of the counter-electrode (and of the electrolyte) the symmetry of the equipotential lines is virtually spherical. Fig. 10 details deviations from spherical symmetry as a function of the ratio between the electrode and electrolyte diameter. Deviations from spherical symmetry are marked at a distance from the electrode about one half the electrolyte diameter.

In the case of A-type cells, as well as types B and C, a value of ρ^0, the resistivity of the corresponding three-dimensional model cell can be calculated using the known value of the cell constant R of the model cell. This in turn can be calculated from the experimental voltage drop across two electrodes of diameter D of a type A cell, at adistance L, by assuming that the electrode area is that of a circle having the same diameter D, so that

$$R = \rho^0 \frac{L}{S} = \rho^0 \frac{L}{(D/2)^2}.$$

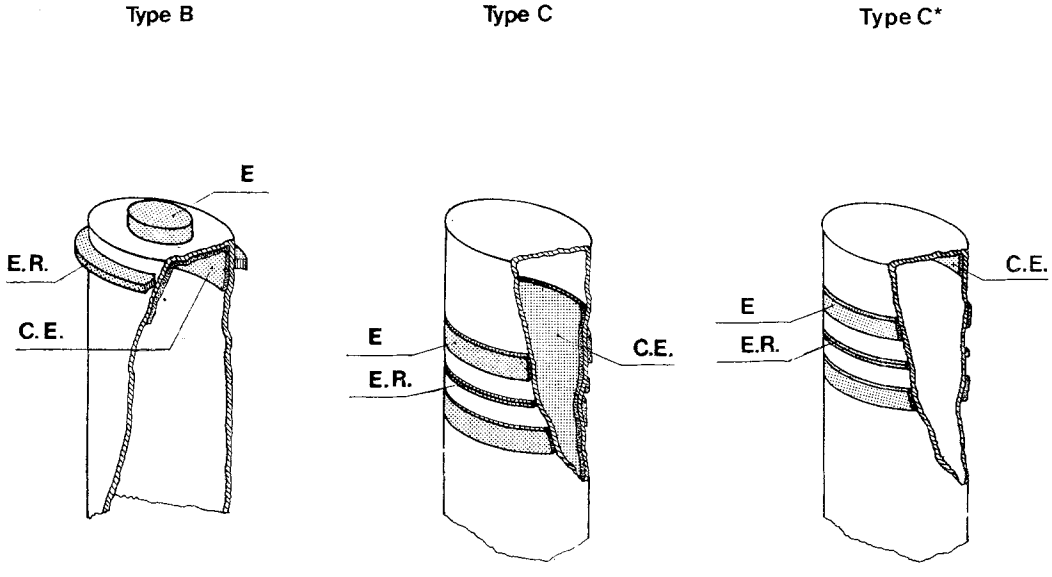

Fig. 3. Different types of electrode arrangements on a tubular-type electrolyte.

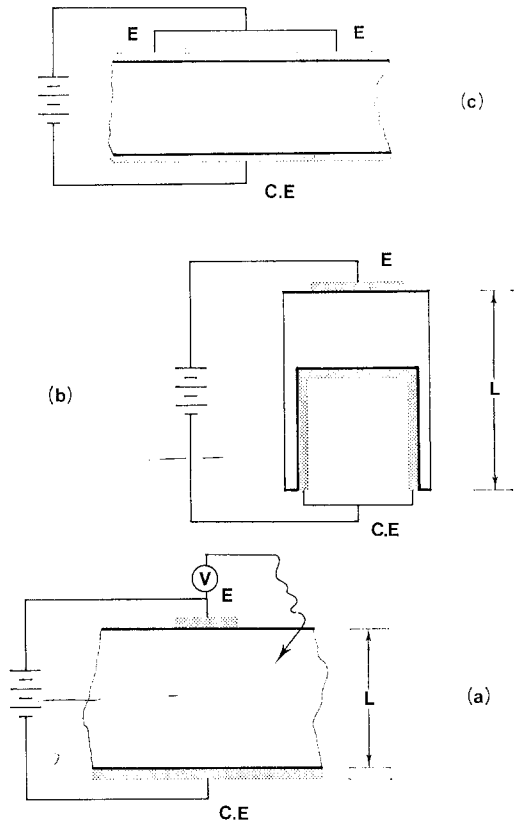

Fig. 4. Experimental layout for measuring equipotential contours on model electrochemical cells.

The value of ρ^0 obtained is $11{\cdot}1 \times 10^3$ Ω cm. This ρ^0 value permits the extension of the results from these present experiments to specific electrolyte systems, having only to allow for the specific resistivity value of the electrolyte and for the current passing in the cell, by writing the ratios:

$$V^0 : 11{\cdot}1 \times 10^3 \, i^0 = V : \rho i$$

where V^0 is the voltage read (in mV) on an equipotential contour; i^0 is the current used in measuring the ohmic drops in the model cells (20 μA); ρ is the specific resistivity of the electrolyte of the real system and i is the current passing in it (μA).

2. In model B cells, where the electrode is on the flat end of the tube, the distribution of the equipotential lines is very similar to that observed on type-A cells and the presence of a discontinuous electrode, which simulates a porous electrode, only affects the absolute values of the ohmic drop.

3. In model cells of the C-type, shown in Figs. 8 and 9, where the electrode is on the outer wall of the tube, the equipotential lines depend strongly on the configuration and position of the electrode relative to the counter-electrode. It is apparent that the type of configuration

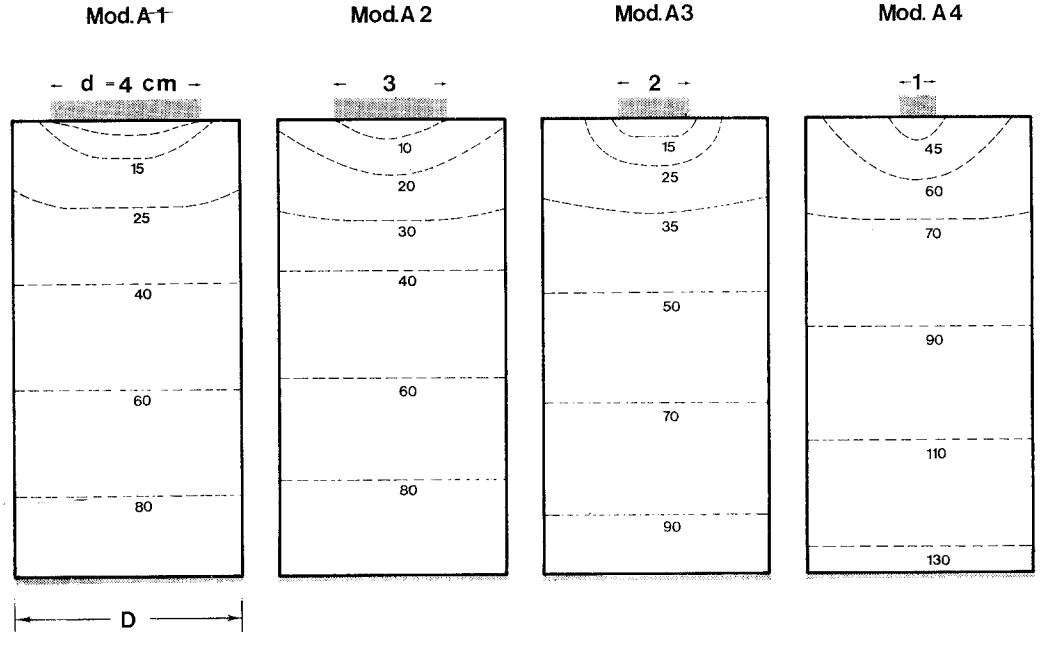

Fig. 5. Equipotential lines for A-type cells.

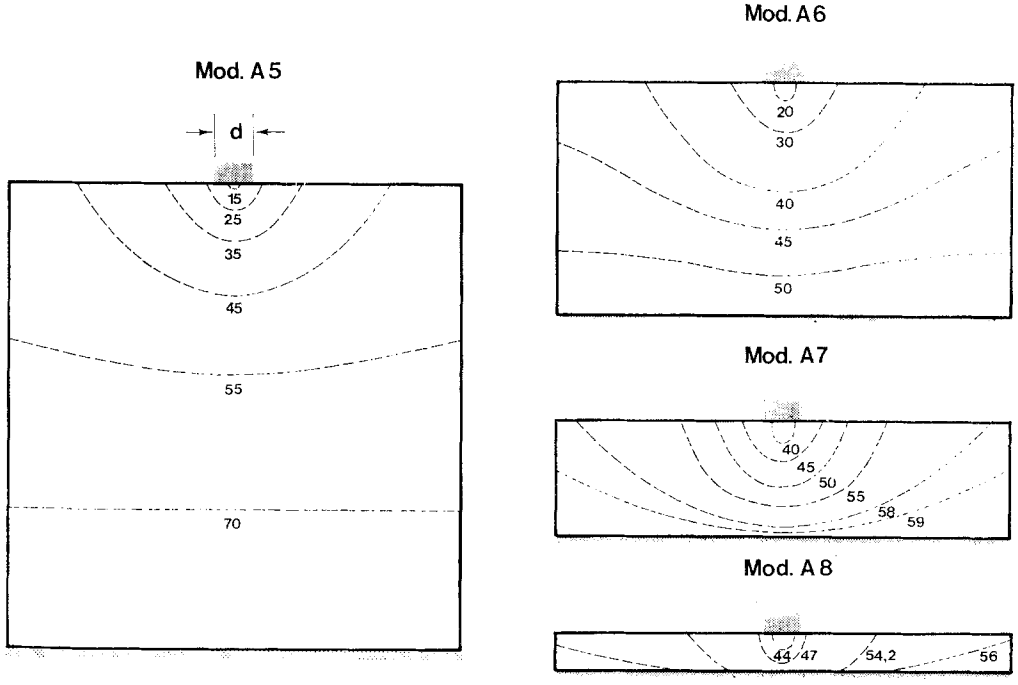

Fig. 6. Equipotential lines for A-type cells.

simulated in type-C_2 cells is very favourable. The reference electrode could be inserted between the two ring electrodes and should experience very little ohmic drop. The results obtained when operating a C*-type of cell are also noteworthy. This has the counter-electrode located in correspondence with the inner flat surface of the electrolyte tube, while the electrode(s) are of the ring type, located on the outer wall of the cylinder. Fig. 9 clearly shows that a preferential current path arises between the counter-electrode and the upper electrode, which could give rise, in a practical situation, to a very inhomogeneous current distribution and exceedingly high current densities in the region of the preferential current path.

The conclusion is that the optimum electrode/counter-electrode configuration should be chosen for each configuration of the electrolyte and with regard to the purpose of the polarization experiment. Great care is required to avoid narrow current pathways, which would give rise to very unrealistic results.

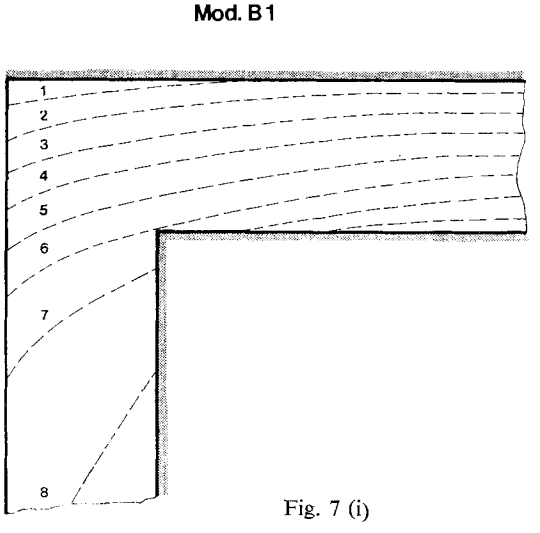

Fig. 7 (i)

3. Comparison of the results on model electrochemical cells with the results of polarization measurements

Some results of anodic polarization experiments are reported, which emphasize the value of the use of model electrochemical cells both for explaining apparently anomalous results and for demonstrating the influence of cell geometry on the measured overvoltage.

Only anodic overvoltage results are considered here, since in the case of cathodic

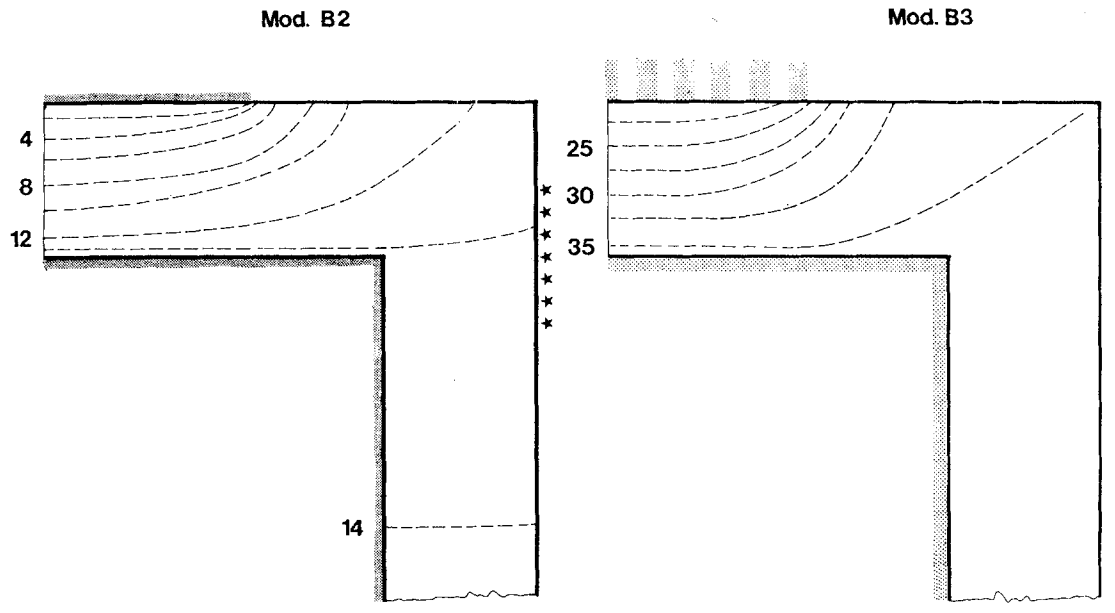

Fig. 7 (i) and 7 (ii). Equipotential lines for B-type cells. These represent half a section of a tube. Original magnification 20 ×.

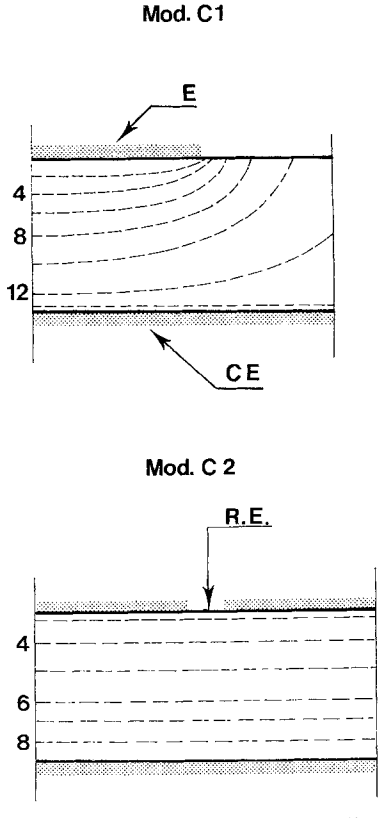

Fig. 8. Equipotential lines for C-type cells. Original magnification 20 ×.

polarization the presence of limiting currents makes the shape of the I–E curves less readily comparable. Polarization measurements have been carried out using an AMEL 551 Potentiostat. The current versus time profiles were recorded with a 0·2 s full-scale deflection, Texas Servowriter II Recorder. The polarization cell, shown in Fig. 11, consisted of one or two porous Pt electrodes (E), a reference electrode (RE) and a counter-electrode (CE) prepared as described in our previous paper [2]. Another type of cell had the Pt electrode on the top of the flat end of the tube, while the reference electrode was located in correspondence with the upper electrode (Fig. 11). Engelhard type 6082 Pt paste was used. This was fired at 600°C and then annealed at 1000°C [2]. The yttria-stabilized tube was fixed by an O-ring fitting (1) on the flange (2), which served to support a silica glass tube, flanged at the lower end and used for control of the atmosphere surrounding the electrode. The cell was heated in a vertical furnace, with a proportional temperature control. Stray voltages, minimized by the symmetric windings of the oven, were suppressed by using a Faraday cage, in the form of a thin Pt layer painted on the external wall of the silica glass tube and earthed.

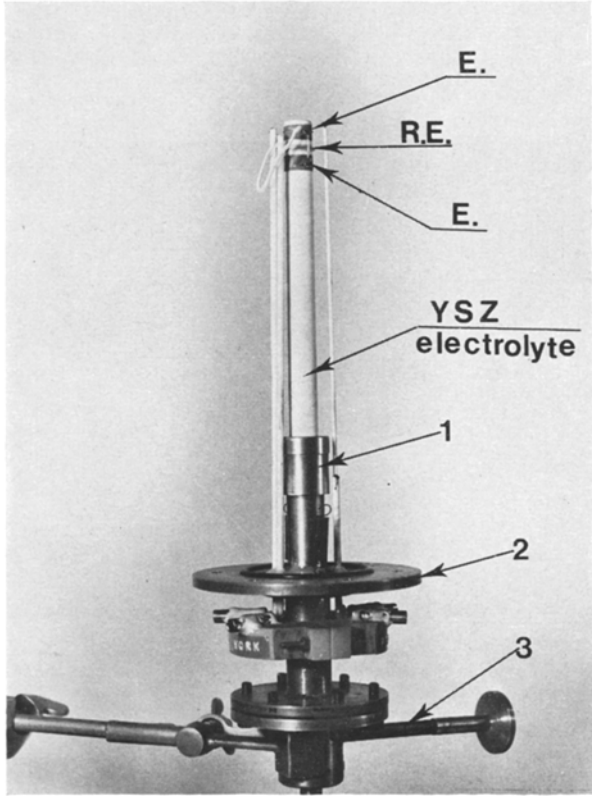

Fig. 11. The three electrode cell used for polarization experiments. E = electrode; RE = reference electrode; (1) = O-ring fitting; (2) = flange; (3) = gas inlet.

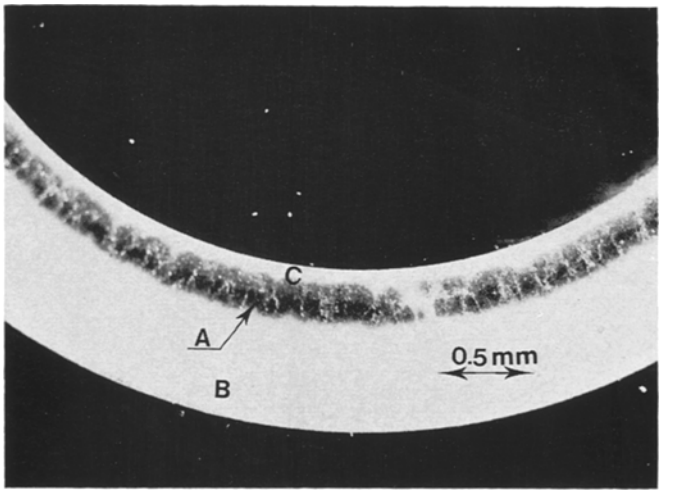

Fig. 16. Crack in a YSZ tube after overnight polarization at 800°C.

facing p. 13

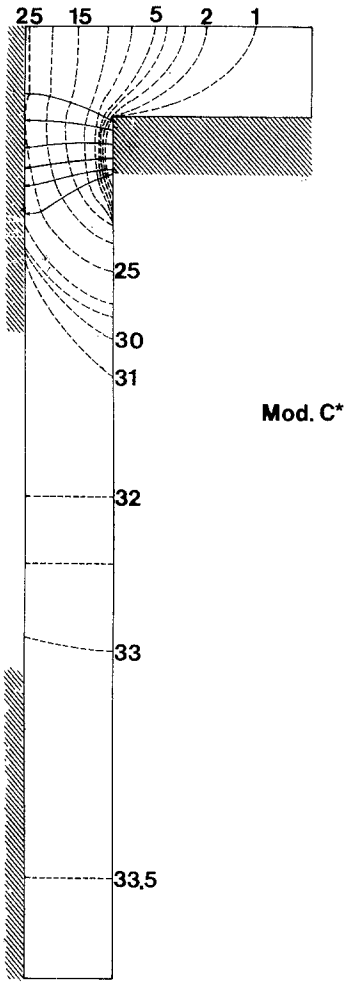

Fig. 9. Equipotential lines for C*-type cells. Original magnification 20 ×.

The first cell configuration experimented with was a B-type cell. Two slightly different arrangements for fitting the current collector to the working electrode were used. This was located as a porous disc, just on the top of the electrolyte (a tube of YSZ of 12 mm diameter), without observing substantially different behaviour.

The first consisted of a Pt disc, held in position on the porous Pt electrode by means of a silica glass disc and springs (Fig. 12a). The second was a Pt wire ring, held in position by a quartz ring and springs (Fig. 12b). Despite the fact that the second electrode fitting permits more easy access and egress of oxygen, no measurable difference was observed in the use of the two configurations.

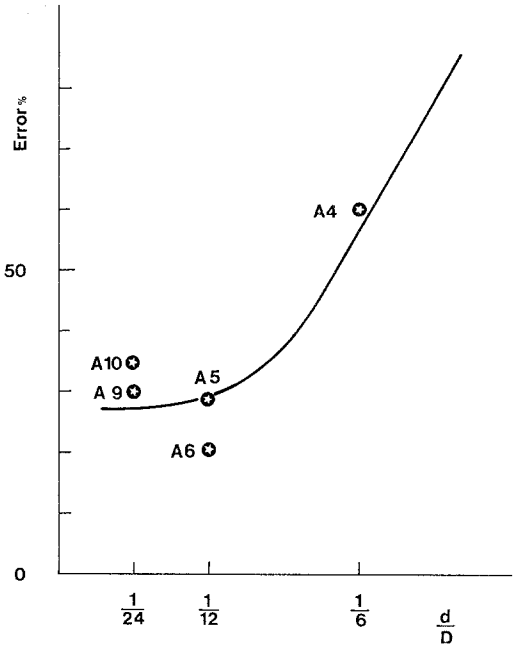

Fig. 10. Calculated deviations from spherical symmetry of the equipotential lines around the electrode in A-type of cells as a function of the ratio d/D.

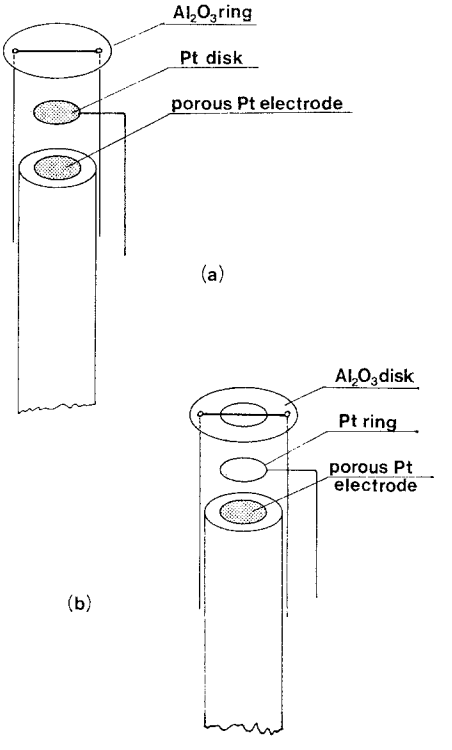

Fig. 12. Arrangement for fitting the current collector to the electrode.

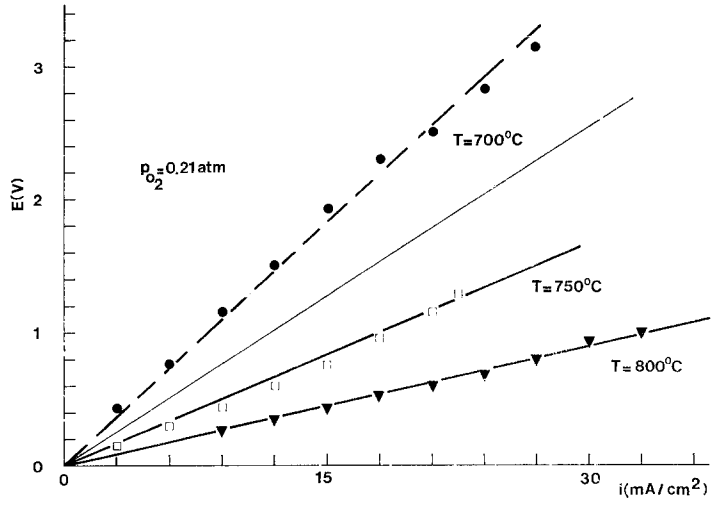

Fig. 13. I–V curves for the anodic polarization of Pt electrodes on type B-cells. Electrode area 0·31 cm², P_{O_2} = 0·21 atm. A Pt ring is used as current collector. Solid lines: IR drops calculated from the value of the cell resistance, measured across the electrode and the counter-electrode by AC bridge.

Analysis of the B-type cells shows (Fig. 7 (ii)) that the reference electrode could be easily located on a group of equipotential lines (indicated by the row of stars) which closely correspond to that lying at the interface between the electrolyte and the counter-electrode. The ohmic drop, therefore, could be readily calculated from the known value of the cell resistance, measured with the AC bridge across the electrode and the counter-electrode. Small errors in positioning the reference electrode do not influence the accuracy of the comparison between the calculated and measured ohmic drop across the electrode and the reference electrode, as an error of $\pm 8\%$ is estimated for an uncertainty in the location of the reference electrode of $\pm 3{\cdot}5$ mm.

The few results [4] reported in Fig. 13 show that at sufficiently high temperatures, where overvoltages are negligible, the voltages read across the electrode and the reference fit closely the curves (solid lines) calculated from the known value of the cell resistance. Only at temperatures lower than 750°C do deviations

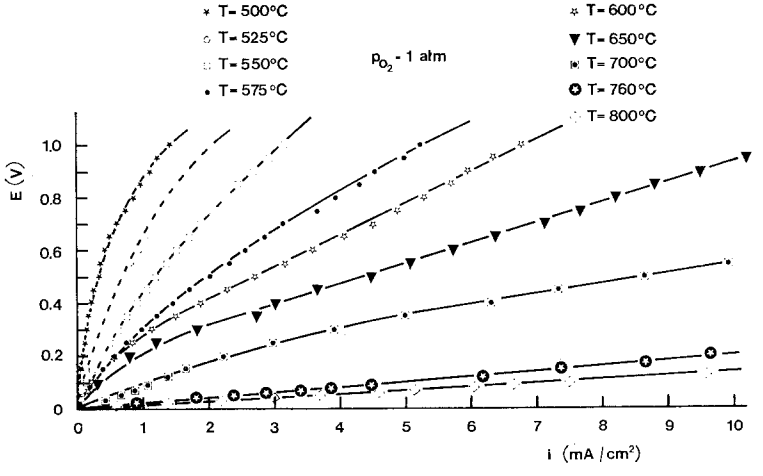

Fig. 14. I–V curves for the anodic polarization of Pt electrodes on a C_1-type cell.

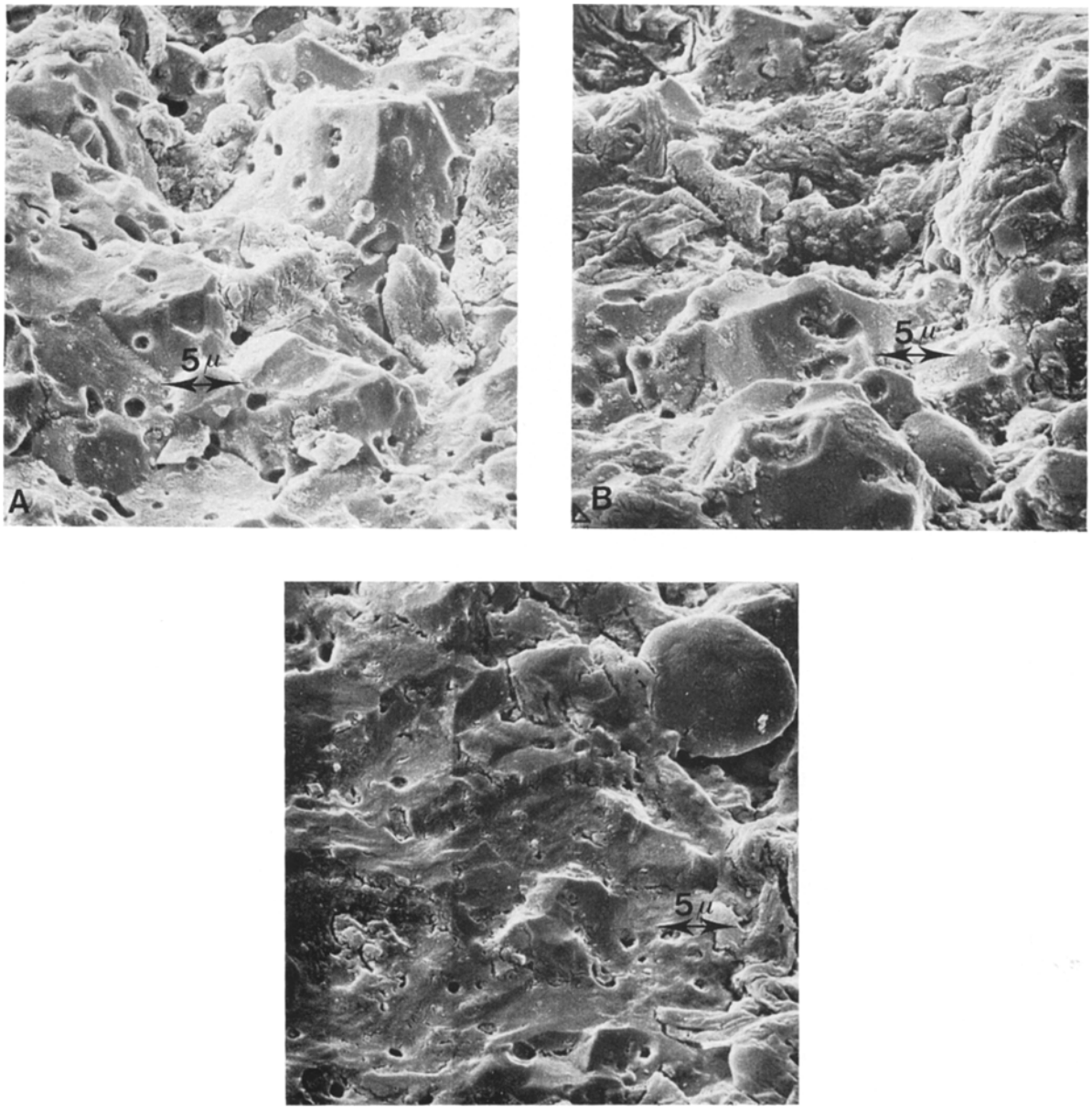

Fig. 17, A, B and C. S.E.M. microphotographs of selected zones along the crack edge in Fig. 16.

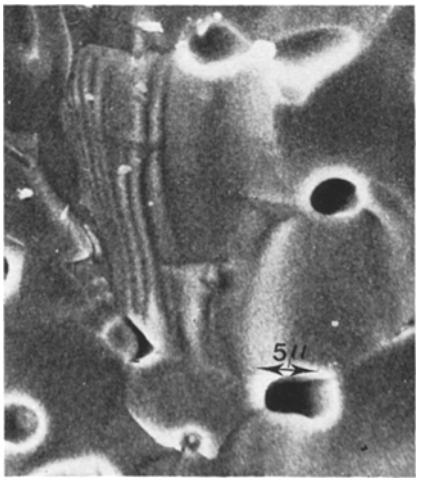

Fig. 18. S.E.M. microphotograph of the section of an undamaged YSZ tube.

facing p. 15

appear, which could therefore be explained entirely as overvoltage terms. This result indicates that with a B-type cell configuration, one might deduce with confidence the overall overvoltage read from the ohmic drop contributions. It is, moreover, notable that the anodic evolution of oxygen above 750°C occurs without appreciable overvoltage, at least up to 30 mA cm^{-2}.

Results dealing with C_2-type cells (one ring electrode, one ring reference electrode) are reported in Fig. 14. These show, in good agreement with previously reported results, that at temperatures in excess of 750°C anodic oxygen evolution occurs at porous Pt electrodes without overpotential. At temperatures below 750°C the curves eventually tend to straight lines, outside a region of current densities within which the electrode reaction occurs with an appreciable overvoltage.

One possible explanation for this tendency is the growth of a platinum oxide layer on the surface of the electrode, which limits the overall rate of the reaction. Complex admittance measurements carried out by Schouler [12] support this view.

The comparison reported in Fig. 15 is of results obtained from a C*-type cell, in one with the two outer ring electrodes connected in parallel and in the other with only the upper electrode used. In both cases the experimental points fit the same I–E curve, provided the measured current (and not the current density) is plotted against polarization voltage, E.

In this case the overvoltage reflects purely ohmic drops despite the fact that Fig. 14 indicates that at this temperature a considerable overvoltage is present. The conclusion is in agreement with the results on model cells (Fig. 9) that a preferential current path is present. As a consequence of local strong Joule heating in the region of preferential current flux the temperature is considerably higher than outside this region and therefore the overvoltage might be lower than that expected. After long-term operation the cell ruptured at the region where Fig. 9 indicates the existence of the preferential current path. This was assisted by reverse polarization at 50 mA overnight.

Fig. 16 is a microphotograph of the crack; near the edge on the cathode side, the electrolyte is blackened and then partially reduced. Figs. 17, A, B and C are scanning electron microscope pictures which show that also outside the black zone an intergranular attack has taken place with the additional formation of small pits in the middle of the black zone. A comparison of these pictures with a section of a tube of YSZ (Fig. 18) which had been used only under normal conditions, as in the preceding experiments, demonstrates that the loss of mechanical strength could be attributed to preferential reduction at grain boundaries or to preferential re-oxidation along grain boundaries, in the case of electrolyte conditioning after reverse polarization.

4. Conclusions

The use of model electrochemical cells has been

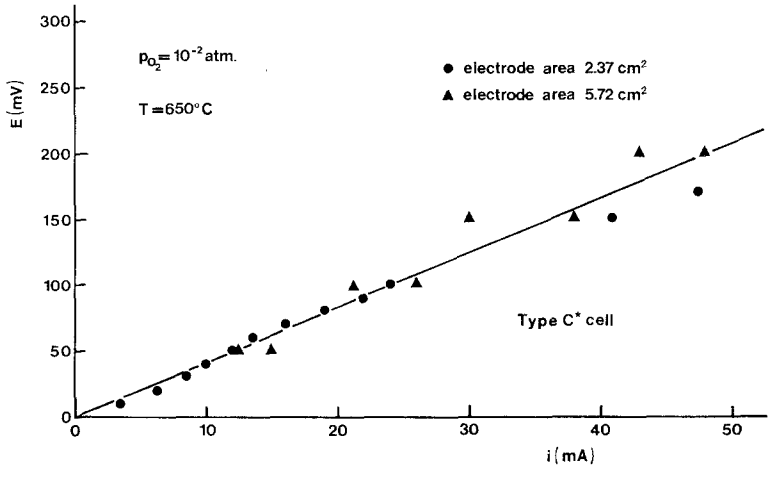

Fig. 15. I–V curves for the anodic polarization of a C*-type of cell.

found to be a very useful tool, which provides information on the feasibility of the safe operation of a cell with a certain configuration or the means for the design of the proper electrode/reference electrode/counter-electrode configuration for any kind of electrolyte configuration which could be handled with a two-dimensional section. It has been also shown that the anodic overvoltage at Pt electrodes is negligible only in excess of 750°C. The use of a counter electrode as reference must be therefore avoided.

Acknowledgements

The authors are indebted to Professor G. Bianchi and Professor W. van Gool for stimulating discussions. This work has been sponsored by the National Research Council, C.N.R., Technology Committee, with Research grant No. 71.01156. 11115.A. 17.

References

[1] S. Pizzini, 'Proc. Symp. Fast Ionic Diffusion', Ed. W. van Gool, North Holland Publ. Co. (1973).
[2] S. Pizzini, M. Bianchi, P. Colombo and S. Torchio, *J. Appl. Electrochem.* **3** (1973) 153.
[3] M. Bianchi, Thesis, University of Milan (1972).
[4] C. Chiesa, Thesis, University of Milan (1972).
[5] R. Piontelli, G. Bianchi and R. Aletti, *Z. Elecktrochem.* **56** (1952) 86.
[6] H. Yanagida, R. J. Brook and F. A. Kroger, *J. Electrochem. Soc.* **117** (1970) 593.
[7] R. J. Brook, W. L. Pelzmann and F. A. Kroger, *ibid.* **118** (1971) 185.
[8] S. V. Karpachev, A. T. Filajev and S. F. Palguev, *Electrochim. Acta* **9** (1968) 1681.
[9] M. Kleitz, Thesis University of Grenoble (1968)
[10] M. Guillou, J. M. Millet and S. Palous, *Electrochim. Acta* **13** (1968) 1441.
[11] J. E. Bauerle, *J. Phys. Chem. Sol.* **30** (1969) 2657.
[12] E. Schouler, Thesis, University of Grenoble (1972).